Eur. Phys. J. D (2016) 70: 199
DOI: 10.1140/epjd/e2016-70226-2

THE EUROPEAN PHYSICAL JOURNAL D

Regular Article

Energy and angular analysis of ejected electrons (6–26 eV) from the autoionization regions of argon at incident electron energies 505 and 2018 eV*

Jozo. J. Jureta[1], Bratislav P. Marinkovic[1,a], and Lorenzo Avaldi[2]

[1] Institute of Physics Belgrade, University of Belgrade, Laboratory for Atomic Collision Processes, Pregrevica 118, 11080 Belgrade, Serbia
[2] CNR-Istituto di Struttura della Materia, Area della Ricerca di Roma 1, CP10, 00015 Monterotondo Scalo, Italy

Received 29 March 2016 / Received in final form 1 August 2016
Published online 13 October 2016 – © EDP Sciences, Società Italiana di Fisica, Springer-Verlag 2016

Abstract. High resolution ejected electron spectroscopy has been used to investigate a large number of Ar autoionizing states producing ejected electrons in the energy range from 6 to 26 eV at impact electron energies of 505 and 2018 eV and ejection angles of 40°, 90° and 130°. The full energy range has been divided into three regions which were analyzed separately. In the first one (6–9 eV) the obtained features are identified as the decay of the Ar^+ satellite states formed above the $Ar^{2+}(^1D)$ at 45.11 eV. In the second one (9–14 eV) all features are identified as due to the decay of excited states formed by the excitation of $3s$ electrons to ns, np and nd subshells. The most prominent features are those arising from the excitation of $3s$ to $nd(^{3,1}D)$. In this series the $3s3p^63d(^1D)$ state with FWHM of 0.040 eV is used as the calibration point for all measured spectra. In the third energy region (14–26 eV) a large number of features is observed. Most of them are identified as the decay of excited states of the type $3s3p^5nl$ and $3s^23p^4nln'l'$.

1 Introduction

Rare gases are the best suited targets to study autoionization processes. Together with helium and neon, argon has been the subject of several investigations by photon absorption and ion and electron impact at different incident energies. For this work we have paid attention to those experimental results from electron impact studies obtained at incident electron energies close to or higher of 500 eV: Simpson et al. [1] at 400 eV with energy resolution 0.1 eV, Ogurtsov et al. [2] at 500 eV and scattering angle of 54.5° within ejected energy range of 6–13.5 eV, Bergmark et al. [3] at several keV, Wu et al. [4] at 2.5 keV and a mean scattering angle of 0°. Unfortunately, these measurements are limited in energies of ejected electrons and do not cover the whole autoionization region. Other measurements with lower incident electron energies have been concentrated on resonance classification, triplet-singlet separation with high resolution and PCI phenomenon [5–9]. Calculations of energy positions of autoionization states have been done by Brion and Olsen [10,11] and Fryar and McConkey [6].

Studies of autoionization states of argon produced by ions have been very rare. Ogurtsov et al. [12] used H^+ ion beam at 20 keV studying the ejection energy region between 5 and 300 eV. Rudd et al. [13] used ion beams of H^+ and Ar^+ of 100 keV. Both measurements had been done with low resolution.

The first studies of resonances in autoionization region of argon by photons have been done by Madden et al. [14] and Samson [15]. In the work [14] many resonances have been observed in the photon energy region of 20–150 eV produced by excitation of a single $3s$ electron to states with the configuration $3s3p^6np$, the excitation of two of the outer $3p$ electrons to states with the configuration of $3s^23p^4nln'l'$ and by the simultaneous excitation of $3s$ and $3p$ electrons to states with the configuration $3s3p^5nln'l'$. Studies by synchrotron radiation have been very extensive. Hall et al. [16] studied near threshold photoionization of argon in the region 32–49 eV of photon energy. They investigated satellite states over the energy range from zero to 1 eV above their respective thresholds. Satellite states occur when one electron is ejected and another is raised to an unfilled orbital in ion state Ar^+, $3s^23p^4nl$. Wills et al. [17] used synchrotron radiation and photoelectron spectroscopy in order to study the $3s^23p^4nln'l'$ doubly excited neutral states in the energy range from 31 to 42.3 eV. Cvejanović et al. [18] investigated the satellite states by using high resolution threshold photoelectron spectroscopy and synchrotron radiation

* Contribution to the Topical Issue "Advances in Positron and Electron Scattering", edited by Paulo Limão-Vieira, Gustavo García, E. Krishnakumar, James Sullivan, Hajime Tanuma and Zoran Petrović.

[a] e-mail: bratislav.marinkovic@ipb.ac.rs

in the photon energy region of 32–51 eV. The satellite states were systematically studied by Kikas et al. [19] by photoelectron spectroscopy at 100 eV photon energy.

A comprehensive analysis of autoionizing levels of argon excited by low-energy heavy-ion impact has been performed by Jørgensen et al. [20]. They recorded energy spectra of 5–20 eV ejected electrons from autoionizing argon states obtained in collisions with several neutral and ionic species. By applying the Wigner spin conservation rule and molecular-orbital diagrams they have been able to interpret the changes in spectra coming from the variation of atomic number or charge state of the projectile and assign the resulting configurations.

The ground state configuration of argon is $1s^2 2s^2 2p^6 3s^2 3p^6$. The first Ar^+ ionic state has the configuration $3s^2 3p^5(^2P_{3/2,1/2})$ at 15.76 and 15.94 eV respectively, with a spin-orbit splitting of 0.180 eV. The first excited $3s$ state has the configuration $3s3p^6(^2S_{1/2})$ at 13.48 eV with ionization threshold, known as M_1 edge, at 29.24 eV (13.48 + 15.76). The first excited ionic $3p$ state at 16.40 eV has the configuration $3s^2 3p^4(^3P)3d(^4D)$. The Ar^{2+} ionic state has three configurations $Ar^{2+}(^3P)$ at 43.375 eV, 43.513 eV and 43.570 eV, $Ar^{2+}(^1D)$ at 45.111 eV and $Ar^{2+}(^1S)$ at 47.498 eV. With incident electron energies of 505 and 2018 eV it is possible to excite and ionize all valence and inner shell electrons i.e. the $3s$, $3p$, $2s$ and $2p$ ones. The $2p$ shell has two sub shells, namely the $2p_{3/2}$ one at 248 eV and $2p_{1/2}$ one at 250 eV known as L_3 and L_2 edges. The $2s$ shell at 327 eV is known as L_1 edge [21]. In the present paper we will be concentrated on ejected electrons obtained by the excitation of $3s$ and $3p$ electrons only. Excitation of L_1, L_2 and L_3 shells will be presented in a forthcoming paper. Excitation of $3s$ electron by electron impact above the first ionization potential can populate the $3s3p^6n(s,p,d)$ autoionizing states, which decay to Ar^+. Excitation of $3p$ electron populates autoionizing states with configuration $3s^2 3p^4 nln'l'$, while the simultaneous excitation of $3s$ and $3p$ electrons leads to states with configuration $3s3p^5 nln'l'$. In all excitation processes the decay to the Ar^{2+} $3p^5$ states can follow 2 channels, therefore one can expect two series of excited states separated by the spin-orbit splitting of 0.180 eV.

In this paper we present high resolution ejected electron spectra of argon in the ejected energy range of 6–26 eV. This ejected energy range was tentatively divided into three energy regions (6–9 eV), (9–14 eV) and (14–26 eV) which are separately discussed. The first region is the region of Auger satellite states of the type $3s3p^5nl$ that decay to the Ar^{2+} ground or excited states. The second region is characterized by the single excitation of $3s$ electron to ns, np or nd subshells of the type $3s3p^6$ (ns, np, nd) with energy limit at 29.24 eV. The third energy region is recognized as the region of the double excitation of the type $3s3p^5 nln'l'$ and $3s^2 3p^4 nln'l'$. The spectra have been measured at the constant incident electron energies of 505 and 2018 eV and three ejection angles of 40°, 90° and 130° with respect to the incident electron beam in order to show angular behavior of the excited states. The systematic angular behavior (10° to 130°) of the states observed from 6 to 12.5 eV of ejected electron energies has been presented at incident electron energy of 505 eV. Also, the feature in cusp like form which corresponds to the ionization potential of $3s$ state (29.24 eV) is present at energies 505 and 2018 eV and three ejection angles 40°, 90° and 130°. The present systematic study of autoionizing states in argon is a continuation of our work [22] of the phenomena connected to the autoionization and Auger processes in rare gasses at higher electron energies.

2 Experiment

The apparatus used in the present measurements has been described in an earlier publication [23]. It consists of a high energy (10–2500 eV) unselected electron gun that can be rotated in the angular range 10°–130° around the analyzer axis, a high resolution hemispherical analyzer with a mean radius of 125 mm and 7 channeltrons for the detection of ejected electrons. After preamplifiers the signals were transferred by optical fiber cables to the counter and proceed by data acquisition and evaluation software. The analyzer operates at constant pass energy with defined retarding ratio and defined magnification determined by the two stage 11 element lens system that provides uniform high transmission and acceptance angle of (±1°). The atomic beam is let into the interaction region via a 20 mm long platinum-iridium non biased needle with internal diameter of 0.5 mm in the perpendicular direction to the scattering plane.

The energy resolution of the ejected electron spectra of argon is determined by the energy resolution of the analyzer at mean kinetic energy of 12 eV and Doppler broadening of 0.0071 eV at temperature of 350 K. The FWHM of the narrowest feature in the spectra was 0.040 eV, while usually the resolution was between 0.060 and 0.080 eV. The background pressure in the vacuum chamber was 6×10^{-8} mbar, while the working pressure with argon was 2×10^{-6} mbar. With electron current of ($9-12 \times 10^{-6}$ A) typical accumulation time for most spectra was between 30 and 60 min with energy width of 0.020 eV per channel. The signal to noise ratio was 2 to 7% in the first and third energy region and 27% in the second energy region. The transmission was not uniform in the first energy region (6–9 eV) and all spectra are presented with the background subtracted without normalization of obtained data. Considering the ejected electron energies of interest and the detection angles this background is dominantly coming from electrons produced in the direct ionization/multiple ionization processes which have a continuous energy distribution. The shape and cross sections of this continuum itself, although interesting per se, will not be further discussed here. The subtraction of the background was achieved by a combination of linear and non-linear functions, and it has no influence to the resonance intensity and its shape. As a calibration point for the ejected electron energy scale was used the $3s3p^6 3d(^1D)$ state at 27.48 eV (11.72 eV ejected

electron energy) in a spectrum of argon and helium mixture at 303 eV of incident electron energy using the energy position of the double excited $2s2p(^1P)$ state in He at 60.130 eV (35.55 eV of ejected electron energy) [24] as a reference. The incident electron energy scale was calibrated through the elastic channel.

3 Results and discussion

3.1 The first ejected energy region from 6 to 9 eV

This ejected energy region is populated by several well defined isolated features shown in Figures 1a and 1b with corresponding energies and assignments presented in Table 1. The features have been obtained at constant incident electron energies 505 and 2018 eV and ejection angles 40°, 90°, and 130°. In comparison with the neon ejected spectra [22] the number of feature is less and they are present with lower intensities. The excited states which produce these ejected electrons belong to the energy region of the Ar^+ satellite states measured in photoionization experiment ([19] and references there in). Identification of these states was made according to their ejected energies and their absence in the spectra taken below 50 eV of incident electron energy. All states are produced by excitation of Ar^+ $3s3p^5nl$ states embedded in the $Ar^{2+}(^3P, ^1D, ^1S)$ continua. The features present in the spectrum are due to the decay to these ion states, preferentially to (^1D) state at 45.11 eV. Decays to other two states (^3P) and (^1S) have not been identified.

The ejected energy of the first feature (A) at 6.22 eV is in good agreement with previous works [12,13,25]. The feature has been observed for the first time by Rudd et al. [13] and Ogurtsov et al. [12] in collision by fast ions, while in low electron energy collision the feature was observed by Hicks et al. [25]. The assignment of this feature until now is not clearly defined. For Rudd et al. [13] the origin of this feature was unknown, but they noticed a higher intensity of the feature in the collision with fast H^+ ions than with Ar^+ ions. Ogurtsov et al. [12] assigned this feature to an autoionizing state of the form $3s3p^54s4p$ with excitation cross section of the order of 10^{-19} cm^2. In the photoionization experiment by Kikas et al. [19] the feature is assigned as a satellite state of the form $3s^13p^5(^3P)3d$ because it is strongly enhanced in the decay spectrum of the $2p^53d$ states with FWHM of 0.157 eV. Hicks et al. [25] did not assign the feature, but proposed energy position of 53 eV, suggesting that it corresponds to an Ar^+ state which decays through electron ejection to an Ar^{2+} state at about 47 eV. In the present experiment the feature is well defined with a FWHM of about 0.070 eV showing the same lineshape at the three ejection angles indicating that it belongs to an Auger state. The excellent agreement in energy position with line 73 from Kikas et al. [19] has been the argument to accept the assignment proposed by these authors. The same argument has been applied to accept the assignment for the feature (D) at 52.81 eV (7.70 eV of ejection energy). Again, a good agreement in energy position was found with the satellite line 75 at 52.84 eV in photoionization experiments [19,26]. The FWHM of the feature (D) is about 0.060 eV and the form of the feature does not show any angular dependence. The intensity ratio between features (A) and (D) at 505 eV in Figures 1a is 1.97 for 40°, 2.48 for 90° and 2.19 for 130°. The feature (F) at 53.73 eV (8.62 eV of ejection energy) is in excellent agreement with energy position of the satellite line 77 at 53.74 eV in [19,26]. All other features from Figures 1a and 1b are present with lower intensities and some of them

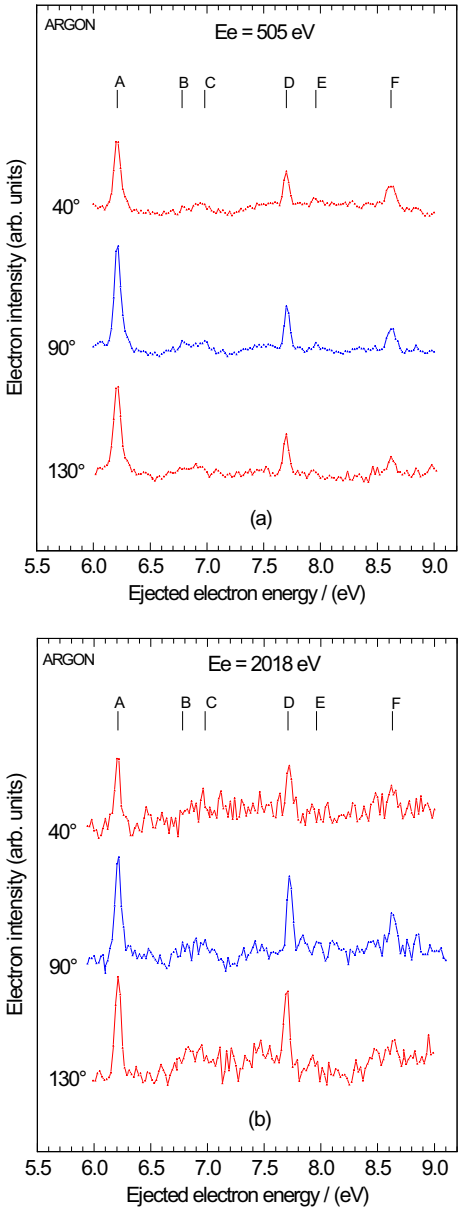

Fig. 1. Two series of ejected electron spectra of argon obtained at three ejection angles of 40°, 90° and 130° and constant incident electron energies of (a) 505 eV and (b) 2018 eV. The energy region of ejected electrons is from 6 to 9 eV with energy width of 0.020 eV per channel. The spectra are shown with subtracted background and without normalization of measured data. The calibration energy for ejected energy scale was energy position of the $3s3p^63d(^1D)$ state at 11.72 eV (27.48 eV).

Table 1. Ejected (in parenthesis) and excitation electron energies (eV) of the features (A to F) observed in the first ejection energy region 6–9 eV.

This work Label	Ref. [19] Line	Ref. [26]	Ref. [25]	Ref. [13]	Ref. [12]	Assignment
(A) (6.22)	73		(6.24)	(6.00)	(6.21)	
51.33	51.36	51.4				$3s^1 3p^5(^3\mathrm{P})3d$
(B) (6.78)						
51.89						
(C) (6.98)						
52.09						
(D) (7.70)	75					
52.81	52.84	52.9				$3s^1 3p^5(^1\mathrm{P})4p(^2\mathrm{S})$
(E) (7.96)						
53.07	53.05					
(F) (8.62)	77					
53.73	53.74	53.8				$3s^1 3p^5(^3\mathrm{P})4d + (^1\mathrm{P})3d$

completely disappear at 2018 eV. They are left without assignments in Table 1 because there are neither enough details for their interpretation nor other measurements for comparison. It is however reasonable that they should belong to the same type of excitation as the other intense features (A, D and F). Only for the feature B at 6.78 eV we could speculate that the final state is the $3s^2 3p^4(^1\mathrm{S}_0)$, at 4.124 eV above the second ionization limit. This would lead to an excitation energy of 54.30 eV in accordance with line 78 in reference [19]. Unfortunately the configuration of this state has not been assigned in reference [19].

3.2 The second ejected energy region from 9 to 14 eV

The ejected energy region from 9 to 14 eV (24.76 to 29.76 eV of excitation energies) is characterized by a wealth of features as shown in Figures 2a–2c. These ejected electrons come from the $3s3p^6nl$ excited states decaying to Ar^+3p^5. All autoionizing states result from the excitation of $3s$ electron to the ns, np and nd subshells. This energy region was studied systematically by electron impact only by few authors [5,6,10,11]. Brion and Olsen [10,11] calculated the energy positions of the states, but the experimental spectra were obtained with rather poor resolution. The resolution presented in [5] was much better but not enough to separate the singlet and triplet states, while in [6] the resolution was enough to resolve the singlet-triplet splitting but with very poor signal to noise ratio. In the photoabsorption work [14] only optically allowed states are detected as resonances in the $3p$ photoionization cross section. In the experiment by ions [12] this energy part had not been studied in details, although later the same group of authors [2] presented spectra with the resolution good enough to demonstrate the singlet-triplet separation, again without detailed analysis. Moreover, the two published spectra display different shapes.

In Figures 2a and 2b we present this part of the ejected electron spectrum obtained with the best signal to noise ratio but with resolution of 0.060 to 0.080 eV, while in Figure 2c the spectra have been measured with the best ever reached resolution of 0.040 and 0.045 eV. Taking into account the large number of observed states we present our results in three separate subsections and Tables 2–4.

3.2.1 Excitation of 3s electron to the 3s3p6ns(^{3,1}S) states

Figures 2a and 2b show the ejected electron spectra obtained at constant incident electron energies at 505 and 2018 eV and at three ejected angles of 40°, 90° and 130°, while Figure 2c shows spectra obtained at 505 eV and two ejection angles of 90° and 130°. Table 2 lists all energies for measured $3s3p^6ns$ features and shows the comparison with other references.

The $3s3p^6ns(^{3,1}\mathrm{S})$ states correspond to features with low intensities labeled by numbers (0) to (6) in order to distinguish them from the $3s3p^6nd(^{3,1}\mathrm{D})$ states. Their identification in Table 2 is made according to their ejected energies and the comparison with previous literature. They belong to optically forbidden states and they can be seen with higher intensities at low incident electron energies. In the past the identification of the $4s(^3\mathrm{S})$ state has been challenging. In the energy-loss experiment [9] close to the threshold (0.26–10 eV) the $4s(^3\mathrm{S})$ state was identified at 25.03 eV with an energy width of 0.080 eV. This energy position is in very good agreement with other two previous works [7,8]. Unfortunately, there are no data on this feature from high incident electron energies. Due to the high resolution in our experiment we were able to identify two features (0) and (1) in the spectra in Figures 2a–2c and assign them as the first members of the ns series. The feature (0) in the form of the shoulder of a broad peak has the energy of 25.02 eV which is in excellent agreement with [7–9] but appears only in the spectra at 40° and 90° ejection angles. The feature is identified as the $4s(^3\mathrm{S})$ state. The next asymmetric feature in the spectrum is peaked at the energy of 25.20 eV, in reasonable agreement with other previous measurements reported in Table 2 [3,5,10]. It has been identified as the $4s(^1\mathrm{S})$ state due to energy separation of 0.180 eV from the $4s(^3\mathrm{S})$ state and very good agreement in energy

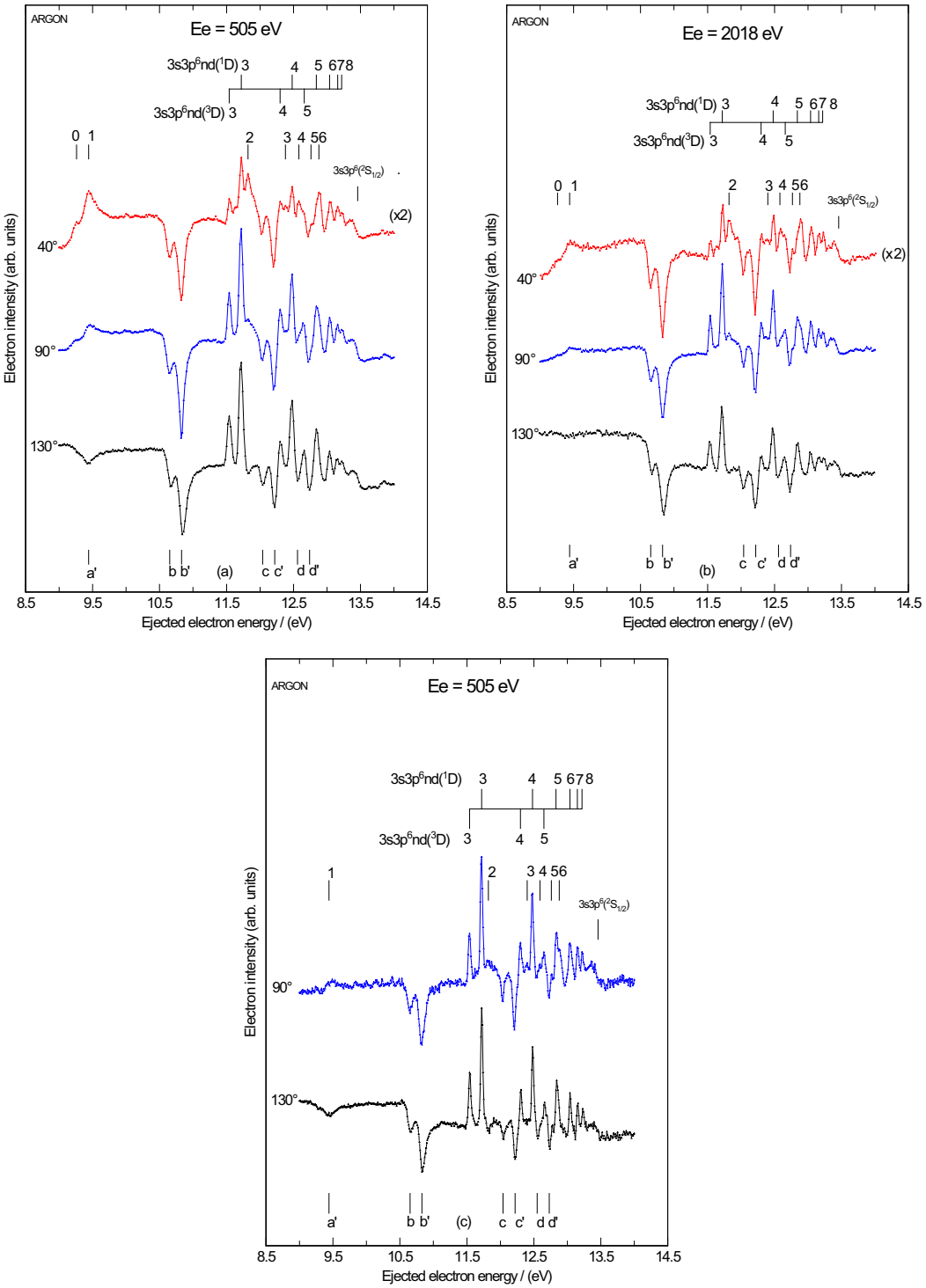

Fig. 2. (a) Ejected electron spectra of argon obtained at constant incident electron energy of 505 eV at three ejection angles 40°, 90° and 130° respectively. Each spectrum was composed from several spectra in order to get reasonable signal to background ratio. The energy region of ejected electrons is from 9 to 14 eV (24.76 to 29.76 eV of excitation energy) with energy width of 0.020 eV per channel. The spectra are shown with subtracted background and without normalization of measured data. The calibration energy for ejected energy scale was energy position of the $3s3p^6 3d(^1\mathrm{D})$ state at 11.72 eV (27.48 eV). Short connected vertical lines above the spectra show energy positions of the features, while short vertical lines at the bottom of Figure show energy positions of minima classified as resonances. The small numbers from 0 to 6 show excitation to $ns(^{3,1}\mathrm{S})$ states. (b) The same as in Figure 2a but for the constant incident electron energy of 2018 eV. (c) Two high resolution ejected electron energy spectra of argon obtained at constant incident electron energy of 505 eV and two ejected angles of 90° and 130° respectively. The FWHM was 0.040 eV for the spectrum at 130° and 0.045 eV for the spectrum at 90°. The spectra are presented with subtracted background without normalization of data with energy width of 0.010 eV per channel.

Table 2. Ejected (in parenthesis) and excitation energies in (eV) of the autoionzation states of argon obtained from excitation of $3s$ electron to the $3s3p^6ns$ states in ejected energy region from 9 to 14 eV (24.76 to 29.76 eV of excitation energies) at incident electron energies of 505 and 2018 eV and three ejection angles 40°, 90° and 130°. Comparison with other experimental results obtained at different incident electron energies and calculations.

This work Label	Ref. [6] (exp.)	Ref. [6] (calc.)	Ref. [10] (calc.)	Ref. [7]	Ref. [3] (calc.)	Ref. [8]	Ref. [5]	Ref. [4]	Ref. [1]	Ref. [9]	Ref. [27]	Assignment $3s3p^6ns(^{3,1}\mathrm{S})$
(0): (9.26) 25.02	25.02			24.96		25.02				25.03		$4s(^3\mathrm{S})$
(1): (9.44) 25.20	25.27		25.22	25.25	25.22	25.26	25.19	25.25	25.8		25.17	$4s(^1\mathrm{S})$
(2):(11.82) 27.58		27.52	27.51		27.59		27.50	27.55	27.55			$5s(^1\mathrm{S})$
(3): (12.40) 28.16		28.24										$6s(^3\mathrm{S})$
(4): (12.59) 28.35		28.27	28.30					28.33	28.1			$6s(^1\mathrm{S})$
(5): (12.76) 28.52		28.59										$7s(^3\mathrm{S})$
(6): (12.88) 28.64		28.61	28.65									$7s(^1\mathrm{S})$
(7): (13.46) 29.22												I.P.$(3s)$ $3s3p^6(^2\mathrm{S}_{1/2})$

Table 3. The same as in Table 2 but for the excitation of $3s$ electron to the $3s3p^6nd(^{3,1}\mathrm{D})$ states.

This work	Ref. [6] (exp.)	Ref. [6] (calc.)	Ref. [10] (calc.)	Ref. [7]	Ref. [3] (calc.)	Ref. [8]	Ref. [5]	Ref. [4]	Ref. [1]	Ref. [29]	Ref. [27]	Assignment $3s3p^6nd(^{3,1}\mathrm{D})$
(11.54) 27.30												$3d(^3\mathrm{D})$
(11.72) 27.48	27.48		27.57	27.61	27.51	27.63	27.54	27.55	27.55	27.48	27.54	$3d(^1\mathrm{D})$
(12.30) 28.06												$4d(^3\mathrm{D})$
(12.48) 28.24	28.24		28.30		28.27		28.35	28.33	28.1	28.29	28.35	$4d(^1\mathrm{D})$
(12.65) 28.41												$5d(^3\mathrm{D})$
(12.83) 28.59	28.59		28.64		28.62		28.70			28.70	28.70	$5d(^1\mathrm{D})$
(13.04) 28.80		28.79	28.83		28.85							$6d(^1\mathrm{D})$
(13.15) 28.91		28.91	28.94									$7d(^1\mathrm{D})$
(13.22) 28.98		28.99	29.01									$8d(^1\mathrm{D})$

Table 4. The same as in Table 2 but for the excitation of 3*s* electron to the $3s3p^6np(^{3,1}P)$. The $[4s(^1S)$, $(130°)]$ state is added to the table due to its presence in the form of minima.

This work Label	Ref. [6]	Ref. [7]	Ref. [3] [calc.]	Ref. [8]	Ref. [5]	Ref. [4]	Ref. [29]	Ref. [9]	Ref. [14]	Ref. [27]	Assignment $3s3p^6np(^{3,1}P)$ $[4s(^1S)]$
(a′): (9.44) 25.20	25.27	25.25	25.22								$4s(^1S)$ $(130°)$
(b): (10.65) 26.41	26.46			26.41				26.56			$4p(^3P)$
(b′):(10.83) 26.59	26.62	26.60	26.62	26.58	26.60	26.605	26.63		26.614	26.60	$4p(^1P)$
(c): (12.04) 27.80	27.93										$5p(^3P)$
(c′): (12.22) 27.98	27.99		27.997		28.00	27.994	28.02		27.996	27.99	$5p(^1P)$
(d): (12.55) 28.31	(calc.) 28.46										$6p(^3P)$
(d′): (12.73) 28.49	28.49		28.51		28.55	28.509	28.50		28.509	28.51	$6p(^1P)$

position with previous works. The question is why these states show the angular dependence, with the maximum at 40° transformed into the minimum at 130° as seen in Figures 2a–2c and 3a and 3d. This phenomenon is seen for the first time in this experiment at 505 eV and Figure 3d shows more clearly the change of the lineshape. The asymmetric minimum labeled as (a′) (see Tab. 4) has a FWHM of about 0.22 eV indicating that it is probably due to two overlapping features.

The feature (2) is identified as the $3s3p^65s(^1S)$ state according to the energy position which is in excellent agreement with [1,3,4] in Table 2. This feature shows a similar angular behavior as the feature (1) i.e. a transformation from the small peak at 40° to the narrow dip at 130°. The remaining features (3–6) are shown in Figure 2c can be seen only at spectra of high resolution. The feature (3) is only seen in this experiment at 90°. The feature (4) has an energy position which is in good agreement with a previous experiment [4] but not with calculations [6,10]. The last two features (5) and (6) have not been seen in other experiments. It is interesting to note the very good agreement in energy position of feature (6) with the calculated one [6,10].

Finally, the last visible change in the cross section is the cusp like form in Figures 2a–2c and 4a and 4b at 29.22 eV, which corresponds to the ionization of 3*s* electron, the M_1 edge. This ejected energy part of the spectrum is zoomed and shown in Figures 4a and 4b with good signal to noise ratio. Both figures show the end of 3*s* electron excitations similarly to helium [23,28] but at variance with neon [22]. According to the ejected energy calibration the energy position taken at the middle of the step function was found at 29.22 eV which is in a good agreement with the calculated value of 29.24 eV (13.48 + 15.76 eV). This form is typical for higher incident electron energy but not for low incident energy below 40 eV and it was observed for the first time in this experiment. Both figures prove that the cusp does not show any angular dependence.

3.2.2 Excitation of 3s electron to the $3s3p^6nd(^{3,1}D)$ states

The excitation of 3*s* electron to the $3s3p^6nd(^{3,1}D)$ states appears in the ejected energy region from 9 to 14 eV shown in Figures 2a–2c with a series of well-defined peaks with an energy separation of 0.180 eV, the spin orbit splitting of the Ar^+ $3p^5$ states. The figures show six and three features in the form of peaks of the (^{1}D) and (^{3}D) series respectively with their energies collected in Table 3, together with some references for comparison.

The most intense feature in the spectrum corresponds to the excitation of the $3s3p^63d(^1D)$ state (27.48 eV) which produce the peak at the ejection energy of 11.72 eV with FWHM of 0.040 eV in Figure 2c and of 0.060 eV in Figures 2a and 2b. This energy position is in excellent agreement with [6,29], but not with other references as can be seen from Table 3. The superior resolution of the present work removes the doubt that this feature could

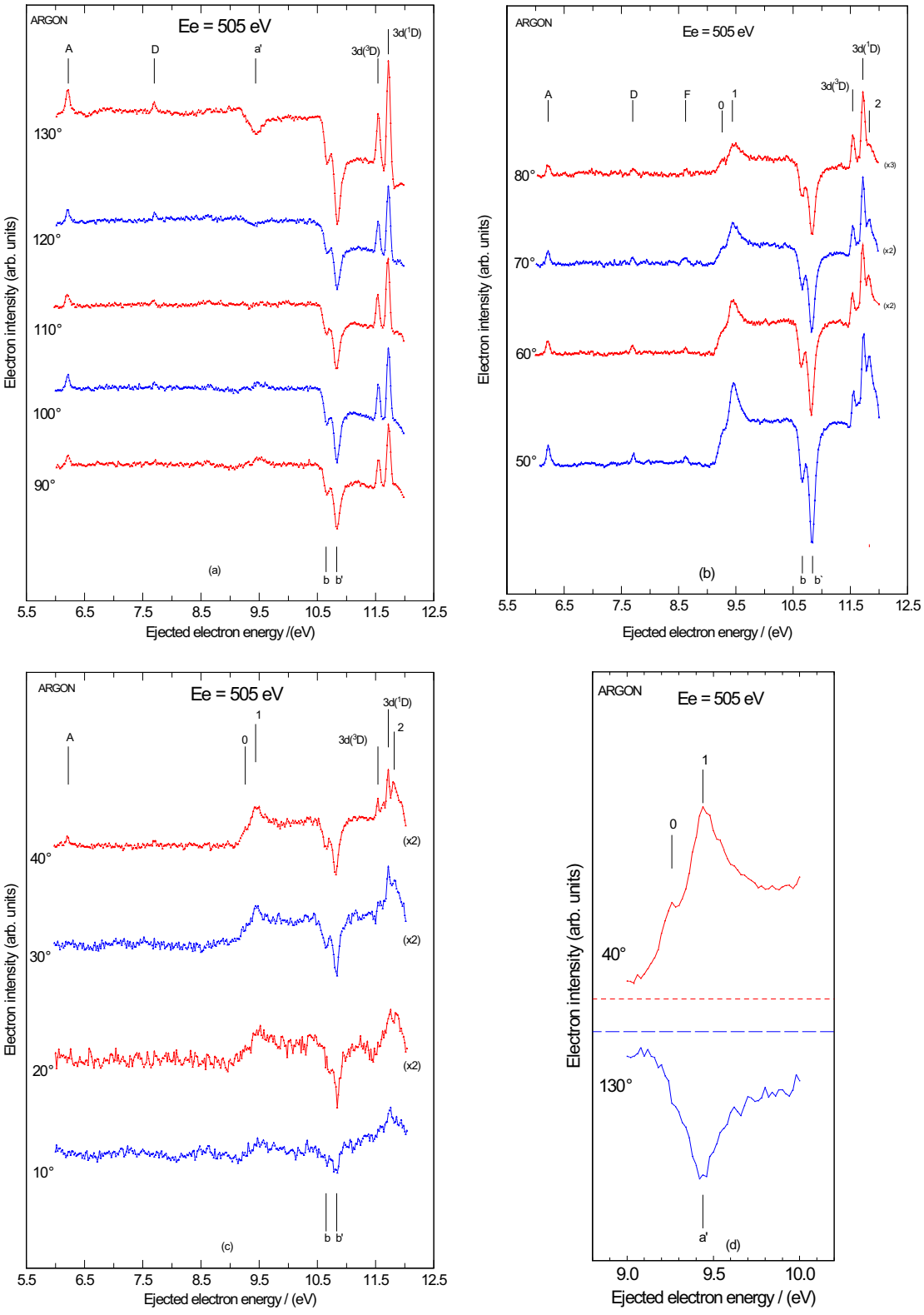

Fig. 3. (a) Several ejected electron energy spectra of argon in the ejection energy region from 6 to 12 eV obtained at constant incident electron energy at 505 eV and ejection angles from 90° to 130° with energy width of 0.020 eV per channel. The spectra are shown with subtracted background and without normalization of measured data. The calibration energy for ejected energy scale was energy position of the $3s3p^6 3d(^1\mathrm{D})$ state at 11.72 eV (27.48 eV). (b) The same as in (a) but for ejection angles from 50° to 80°. (c) The same as in (a) but for ejection angles from 10° to 40°. (d) Part of ejected electron energy spectra of argon obtained at 505 eV and two ejection angles 40° (top) and 130° (bottom) in the ejected energy region of the $3s3p^6 4s(^3\mathrm{S})$ labeled as (0) and the $3s3p^6 4s(^1\mathrm{S})$ labeled as (1) at 40° and marked as (a′) at 130°.

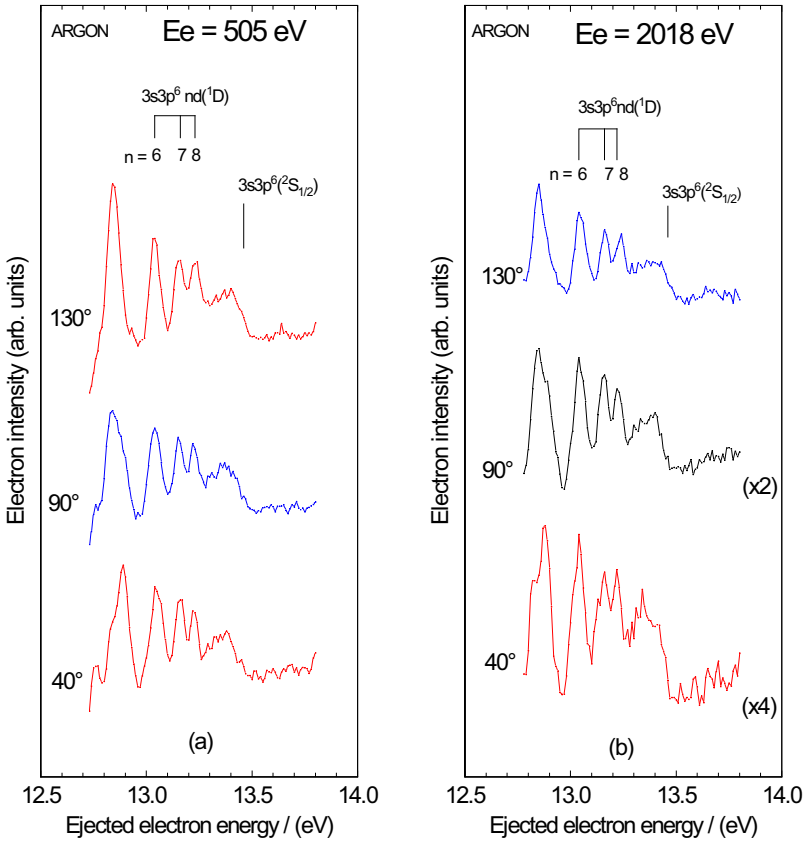

Fig. 4. Part of ejected electron energy spectra of argon obtained at (a) 505 eV and (b) 2018 eV and three ejection angles 40°, 90° and 130° in ejection energy region close to the ionization potential of 3*s* electron $3s3p^6(^2S_{1/2})$ at 29.22 eV known as M_1 edge. Every spectrum is composed from several spectra in order to get satisfactory signal to noise ratio. Energy width was 0.020 eV per channel.

be assigned to the $3s3p^65s(^1S)$ at 27.58 eV. The separation from $5s(^1S)$ state is visible even at 40° where the last feature is present with a shoulder (Figs. 2a and 2b). The feature at ejection energy of 11.54 eV (excitation energy of 27.30 eV) with lower intensity than the $3d(^1D)$ one and separated by 0.180 eV can be assigned to the $3s3p^63d(^3D)$ state. For this state there are no previous references for comparison. The situation is similar for two other triplet states, the $4d(^3D)$ and $5d(^3D)$ ones at 28.06 and 28.41 eV, respectively. All other ($n = 6, 7, 8$) features from this series are identified according to their energies as (^1D) states. Their energies are in excellent agreement with calculation [6]. The last recognized feature from this series corresponds to the $n = 8$ member at 28.98 eV, 0.24 eV below ionization potential of the 3*s* state (29.22 eV). The features of the *nd* series do show no angular dependence as far as the lineshape is concerned, but only a change in relative intensity.

3.2.3 Excitation of 3s electron to the $3s3p^6np$ ($^{3,1}P$) states

The excitation of 3*s* electron to the *np* states corresponds to optically allowed transitions and it has been studied extensively in photoabsorption experiments [14,15] In electron impact experiment at low energies close to the threshold, the excitation of 3*s* electrons to the *np* states appears in form of peaks, while at higher incident electron energies these excitations are represented by dips in the spectra. Already at 100 eV of incident energy [27] the minima have been observed and classified as resonances. They proposed the existence of two series of resonances according to the two ionic triplet and singlet channels. In experiment by ions [2] the minima have been found and classified as *np* states. The minima were also observed in electron energy-loss experiment at 2.5 keV incident energy [4] where absolute optical oscillator strengths were determined. This change in the lineshape of the excited states that depends on incident electron energy was the main reason for discrepancies found in energy positions of the 3*p* states in different experiments, indicating the contribution of another mechanism. This is the resonant excitation already observed in the experiment with neon [30], where the enhanced intensity is due to the formation of negative ion.

In the present experiment the excitation of 3*s* electron to *np* states is shown by three series of double dips with energy separation of 0.180 eV that corresponds to the ion triplet-singlet spin-orbit. The series are shown in Figures 2a–2c with all energies quoted in Table 4.

The first pair of dips labeled as (b) and (b′) are identified as resonant excitation of $3s$ electron to the $3s3p^6 4p(^{3,1}\mathrm{P})$ at energies 26.41 eV and 26.59 eV respectively. This doublet resonant lineshape has not been seen earlier in autoionization region of argon at higher incident electron energies, but it supports the idea presented in [27] of existence of two series of resonances in ejected electron spectra which depends on two Ar^+ $3p^5$ ionic states. Energy positions of these two states are in excellent agreement with the results in [8]. These resonances play very important role in determining the exact energy positions of the excited $4p(^{3,1}\mathrm{P})$ states. The exact energy position of the $4p(^1\mathrm{P})$ state can be taken from photoabsorption measurement [14] and from other low energy electron experiments either very close to the threshold or at least 10 eV above the threshold in order to avoid PCI effects. In our earlier experiment with low electron energy at 41.2 eV [31] it was shown that the energy position of the $4p(^{3,1}\mathrm{P})$ are 26.34 eV and 26.52 eV, respectively. These values are different from energies of resonances for 0.070 eV indicating that resonant contribution is dominant process in $3s$ to $3p$ excitation. It is interesting to note the existence of a large discrepancy in energy position of the $4p(^3\mathrm{P})$ state in the present work (26.34 eV) and the one given in [9] (26.56 eV). In order to confirm the existence of resonances we show angular analysis of these two resonances in ejection angular range from 10° to 130° in Figures 3a–3c. Both structures show angular dependence, they have symmetric shape at ejection angles from 20° to 60° and asymmetric shape from 70° to 130° indicating their resonant character.

The next pair of dips labeled as (c) and (c′) are identified as the $3s3p^6 5p(^{3,1}\mathrm{P})$ excited states. They are present with lower intensity but with the same energy separation of 0.180 eV like in previous case. The energy position of the $5p(^3\mathrm{P})$ state at 27.80 eV can be compared with [6] only at 27.93 eV. Unfortunately there are no other references for comparison that would resolve this discrepancy in energy positions. The energy position of the $5p(^3\mathrm{P})$ state from our previous measurement [31] is 27.76 eV with energy difference of 0.040 eV from the dip (c) at 27.80 eV. The next dip (c′) at 27.98 eV is identified as the $3s3p^6 5p(^1\mathrm{P})$ state. This state was measured in other works [3–5,14,27,29] and Table 4 shows excellent agreement in energy positions between present and other measurements. The energy position for the $5p(^1\mathrm{P})$ state from our measurement at low energy [31] is 27.93 eV with energy difference of 0.050 eV from the dip (c′) at 27.98 eV.

Finally, the dips labeled (d) and (d′) are identified as the $3s3p^6 6p(^{3,1}\mathrm{P})$ at energies 28.31 eV and 28.49 eV, respectively. They are present with low intensities with a shape resulting from the overlap with states close to each other. In comparison with other references from Table 4 one can see that the $6p(^3\mathrm{P})$ state was observed only in the present experiment. The calculation made by Fryar and McConkey [6] shows big discrepancy in energy position (28.46 eV) for this state. The $6p(^1\mathrm{P})$ state was observed in other experiments as shown in Table 4 and a good agreement in energy position between all measurements is obtained.

3.3 The third ejection energy region from 14 to 26 eV

This ejection energy region has been studied very rare in literature by electron impact due to difficulties connected to the high background with very low signal of a few percent only. Hicks et al. [25] presented the ejection energy region from 13.5–20 eV without further analysis. They proposed that the structures in this region belong to the double excited $3s^2 3p^4 nln'l'$ states which decay to the ground state of Ar^+. In ion-argon collisions [12] the ejected energy region of 13–16 eV was shown without analysis. The assignments of these double excited states in autoionization spectra of argon are coming from photoabsorption experiment [14], but for optically allowed transitions only. More recently details about this region have been obtained from experiments using monochromatic synchrotron radiation and photoelectron spectroscopy where the satellite states have been studied [17,19, and references there in]. Here we present high resolution autoionizing spectra in argon in ejected energy region of 14–26 eV obtained at constant incident electron energies of 202, 505 and 2018 eV at three ejection angles 40°, 90° and 130°. A large number of structures has been observed. They are presented in Figures 5a–5c with energies quoted in Tables 5–7. In order to get the best signal to noise ratio each spectrum was collected several times under the same experimental conditions. In the final form they are presented with a background subtracted without any normalization of data.

Table 5 shows energy positions of the first 20 features from Figures 5a and 5b and their comparison with two references. The features have been assigned only when the energy is equal or very close to the energies from the listed references. A large number of features stays unassigned and call for other measurements or theoretical calculations. From this work it is clear that all states in excitation energy region of 30–34 eV from Table 5 belong to the excited states below the second ionization potential Ar^{2+} (43–48 eV) and they have to be assigned as optically forbidden states.

In Table 6 the energy positions of another series of features labeled (21) to (40) with excitation energies from 34 to 41 eV are collected. Comparison was made with 6 references from synchrotron radiation experiments. A good agreement in the energy positions for some features of this work and reference [19] exists, thus the assignments proposed by these authors has been accepted. Still, seven features are left without assignment looking for another measurements and theoretical calculations.

Table 7 lists fifteen features which appears as minima in the spectra shown in Figures 5a and 5b and are labeled from (a) to (o). The features have a shape of double dip with energy separation: 0.19 eV (a-b); 0.15 eV (c-d); 0.17 eV (e-f); 0.28 eV (h-i); 0.19 eV (j-k); 0.16 eV (l-m); 0.18 eV (n-o). The energy separations are very close to the energy spin-orbit splitting of the ion (0.18 eV) indicating that they belong to two series of excited states with strong resonant character, like in the case of single excitation of $3s$ electron to the np states (Figs. 2a–2c). This time the comparison is made with [17] only and an excellent

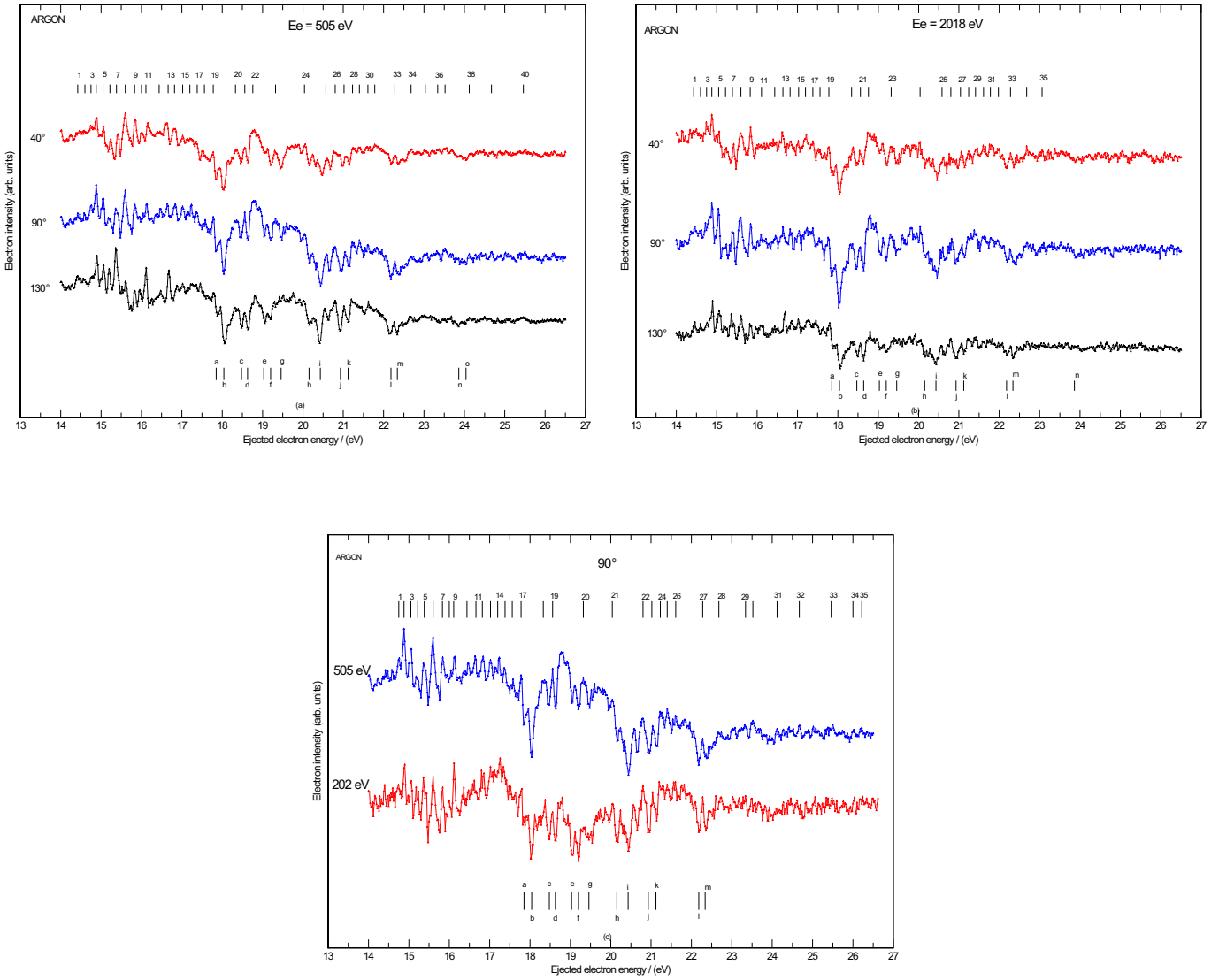

Fig. 5. (a) Ejected electron spectra of argon obtained at constant incident electron energy of 505 eV and three ejection angles 40°, 90° and 130° respectively. Every spectrum was composed from several spectra in order to get reasonable signal to noise ratio. The spectra are presented with subtracted background without normalization of data in ejected energy region from 14 to 26.5 eV. Short vertical lines above spectra show energy positions of features labeled from (1) to (40) presented in Tables 5–7 together with results from other references, while short vertical lines at the bottom of the spectra show energy positions of minima labeled from (a) to (o). The energy width was 0.020 eV per channel. (b) The same as in (a) but for the constant incident electron energy of 2018 eV. (c) Comparison between ejected electron spectra obtained at 505 and 202 eV at fixed ejection angle of 90° in order to show absence of the excitation of $2p$ electrons at 250 eV. The rest is the same as in (a).

agreement in the energy positions between some features has been found. Still seven features are left without assignments. From this work one can conclude that features have resonant character and their excitation energies lie below the second ionization potential of Ar^{2+}. It is interesting to note that there is no correlation between these features and resonances obtained from [36] in metastable excitation functions in doubly excited states region in Ar.

In order to avoid contribution from inner $2p$ shell excitation which start at around 250 eV to excitation spectra in Figures 5a–5c we present comparison of two spectra measured at constant incident electron energies 505 eV and 202 eV in Figure 5c. There is no visible difference between the two spectra; therefore we can exclude an inner shell contribution to the measured spectrum.

4 Conclusions

High resolution ejected electron spectroscopy has been used to study a wide ejected energy range 6–26 eV in autoionization region of Ar at constant incident electron

Table 5. Ejected (in parenthesis) and excitation energies in (eV) from the third autoionization energy region of argon obtained at incident electron energies of 505 and 2018 eV and three ejection angles 40°, 90° and 130°. Comparison with other references.

This work Label	Ref. [14]	Ref. [17]	Ref. [20]	Assignment
(1): (14.43) 30.19	30.23			$(^1\mathrm{D})4s(^2\mathrm{D}_{3/2})4p$
(2): (14.60) 30.36			g 30.39	$(^1\mathrm{D})4s3d(^1\mathrm{D})$
(3): (14.75) 30.51				
(4): (14.88) 30.64	30.65		h 30.69	$(^3\mathrm{P})3d(^2\mathrm{D}_{3/2})4p$
(5): (15.05) 30.81				
(6): (15.22) 30.98				
(7): (15.38) 31.14				
(8): (15.60) 31.36	31.35		J 31.34	$(^3\mathrm{P})3d(^2\mathrm{P}_{1/2})5p$
(9): (15.83) 31.59				
(10): (16.00) 31.76			k 31.74	$(^3\mathrm{P})3d^2$
(11): (16.11) 31.87			l 31.88	$(^3\mathrm{P})3d^2$
(12): (16.44) 32.20		32.18		$(^3\mathrm{P})3d(^4\mathrm{D})$ $(^3\mathrm{P})3d(^4\mathrm{D}_{3/2})$
(13): (16.64) 32.40				$(^3\mathrm{P})4s(^4\mathrm{P}_{5/2})$
(14): (16.82) 32.58			n 32.54	$(^1\mathrm{D})3d4p$
(15):(17.03) 32.79	32.78		o 32.76	$(^1\mathrm{D})4s(^2\mathrm{D}_{5/2})8p$
(16): (17.20) 32.96	32.92	32.95		$(^3\mathrm{P})4s(^2\mathrm{P})$ $(^1\mathrm{D})4s(^2\mathrm{S}_{1/2})10p$
(17): (17.38) 33.14				
(18): (17.56) 33.32				
(19): (17.78) 33.54		33.46		$(^3\mathrm{P})3d(^4\mathrm{F})$
(20): (18.33) 34.09		33.99		$(^3\mathrm{P})3d(^4\mathrm{P})$

energies 505 and 2018 eV and ejection angles 40°, 90° and 130°. The excitation of $3s$ electrons to ns series occur with low intensities. The excitation to $nd(^{3,1}\mathrm{D})$ states is dominant process comparing to the excitation to $ns(^{3,1}\mathrm{S})$ states. However the excitation to $np(^{3,1}\mathrm{P})$ states is present in the form of double minima with energy separation of 0.180 eV, which correspond to the ion singlet-triplet splitting. It is found that the intensity of the $3s3p^64s(^3\mathrm{S})$ state shows angular dependence decreasing from the maximum at 40° to the minimum at 130°. Ionization potential of the $3s$ state is observed as a cusp like feature at the energy of 29.22 eV that does not show an angular dependence. Excitation of $3s$ electrons to the np states is present in the form of double minima with energy separation of 0.180 eV. Their forms indicate the resonant character which was confirmed by angular behaviour from 10° to 130°.

A large number of features has been observed and their energies are presented in several tables and compared with other references. Good agreement was found in comparison with some references from electron, ion and photoabsorption measurements, but some features are left without assignment and they need new measurements and theoretical calculations. A detailed angular dependence

Table 6. Continuation of Table 5 under the same conditions.

This work Label	Ref. [19] Line	Ref. [32]	Refs. [33,34]	Ref. [17]	Ref. [26] Line	Ref. [35] Line	Assignment
(21): (18.56)	4						
34.32	34.36		34.38				$(^3P)3d(^2F_{5/2})$
(22): (18.76)	6				1		$(^3P)3d(^2P)$
34.52	34.50	34.47	34.49		34.5		$(^3P)3d(^2D_{5/2})$
(23): (19.32)							
35.08							
(24): (20.04)							
35.80							
(25): (20.58)	12				3′		$(^1S)4s(^2S)$
36.52	36.52	36.55	36.50		36.52		$(^1S)4s(^2S_{1/2})$
(26): (20.80)							
36.56				36.50			$(^1S)4s(^2S)$
(27): (21.04)							
36.98							
(28): (21.23)	15				3		$(^1D)4p(^2P)$
37.17	37.20		37.19	37.16	37.15		$(^1D)4p(^2P^\circ_{1/2})$
							$(^1D)3d(^2D)$
(29): (21.41)	16						
37.35	37.40	37.40	37.38				$(^1D)3d(^2P_{3/2})$
(30): (21.61)							
37.37				37.41			$(^1D)3d(^2P)$
(31): (21.78)							
37.54							
(32): (21.98)							
37.92							
(33): (22.28)	18						$(^1S)3d(^2D)$
38.04	38.05	38.07	38.03	38.06			$(^1S)3d(^2D_{5/2})$
(34): (22.68)						4	$(^1D)3d(^2S)$
38.44						38.53	$(^1D)3d(^2S)$
(35): (23.06)	21						$(^3P)4d(^4F)$
38.82	38.85	38.86	38.84	38.90			$(^3P)4d(^4P_{1/2})$
(36): (23.34)							
39.10							
(37): (23.52)							
39.28							
(38): (24.12)	27						
40.00	40.06	40.05	40.04	40.07			$(^1D)5s(^2D)$
(39): (24.67)	28						$(^1D)4d(^3D)$
40.43	40.40	40.42	40.38	40.49			$(^1D)4d(^2P,\ ^2G)$
(40): (25.46)	33					5	$(^3P)5d(^2P)$
41.22	41.23	41.22	41.21	41.18		41.15	$(^1D)4d(^2S_{1/2})$

at 505 eV incident electron energy is presented where the ejected electron spectra have been recorded each 10° in the range from 10° to 130°. Especially the angular dependence of the $3s3p^64s(^{3,1}S)$ and the $3s3p^64p(^{3,1}P)$ states has been investigated as well as the angular behaviour of cusp at 13.46 eV.

In comparison with previous measurements this investigation presents the first complete analysis for all single excitation of $3s$ electrons and double excitation of $3p$ electrons. It was found that $3s$ electron excitation to np states was present in form of the features with resonant character.

Table 7. Continuation of the Table 5 under the same conditions.

This work Label	Ref. [17]	Assignment
(a): (17.85) 33.61	33.61	
(b): (18.04) 33.80	33.80	
(c): (18.48) 34.24	34.26	
(d): (18.63) 34.39		
(e): (19.03) 34.79		
(f): (19.20) 34.96	35.00	$(^3\mathrm{P})4p(^4\mathrm{P})$
(g):(19.46) 35.22		
(h): (20.1 5) 35.91	35.95	
(i): (20.43) 36.19		
(j): (20.93) 36.69		
(k): (21.12) 36.88	36.90	$(^1\mathrm{D})4p(^2\mathrm{F})$
(l):(22.18) 37.94		
(m): (22.34) 38.10	38.06	$(^1\mathrm{S})3d(^2\mathrm{D})$
(n):(23.86) 39.62	39.65	$(^1\mathrm{S})4p(^2\mathrm{P})$
(o): (24.04) 39.80		

This paper is dedicated to Prof. Michael Allan in recognition to his crucial contributions to the field of electron scattering and major advancements of experimental techniques. The work has been performed under the project OI 171020 of MESTR of Republic of Serbia and within the scope of bilateral project between Italy and Serbia of particular relevance (Grande Rilevanza) "Nanoscale insights in radiation damage". We acknowledge the partial support of COST Actions MP1002 "Nano-scale insights in ion beam cancer therapy" (Nano-IBCT) and CM1204 "XUV/X-ray light and fast ions for ultrafast chemistry (XLIC)". One of us, J.J.J., is grateful for the financial support of the Innovation Centre of Institute of Physics Belgrade (IPB).

References

1. J.A. Simpson, G.E. Chamberlain, S.R. Mielczarek, Phys. Rev. A **139**, 1039 (1965)
2. G.N. Ogurtsov, I.P. Flaks, V.M. Mikoushkin, S.G. Shapiro, S.I. Sheftel, in *Proceedings of IX International Conference of Physics of Electronic and Atomic Collisions, Seattle, 1975*, edited by J. Sisley and R. Geballe (University of Washington Press, Seattle and London, 1976), p. 767
3. T. Bergmark, R. Spolin, N. Magnusson, L.O. Werne, C. Nandling, K. Siegbahn, Uppsala Univ. Inst. Phys. Report No. 589, 1969
4. S.L. Wu, Z.P. Zhong, R.F. Feng, S.L. Xing, B.X. Yang, K.Z. Xu, Phys. Rev. A **51**, 4494 (1995)
5. J. Peresse, F. Gelebart, A. Le Nadan, C.R. Acad. Sci. Paris Ser. B **275**, 255 (1972)
6. J. Fryar, J.W. McConkey, J. Phys. B **9**, 619 (1976)
7. E. Bolduc, J.J. Quemener, P. Marmet, Can. J. Phys. **49**, 3095 (1971)
8. P. Veillette, P. Marchand, Can. J. Phys. **52**, 930 (1974)
9. D.G. Wilden, P.J. Hicks, J. Comer, Nature **273**, 651 (1978)
10. C.E. Brion, L.A.R. Olsen, J. Phys. B **3**, 1020 (1970)
11. C.E. Brion, L.A.R. Olsen, Chem. Phys. Lett. **22**, 400 (1973)
12. G.N. Ogurtsov, I.P. Flaks, S.V. Avakyan, Sov. Phys. J. Exp. Theor. Phys. **30**, 16 (1970)
13. M.E. Rudd, T. Jørgensen Jr, D.J. Volz, Phys. Rev. **151**, 28 (1966)
14. R.P. Madden, D.L. Ederer, K. Codling, Phys. Rev. **177**, 136 (1969)
15. J.A.R. Samson, in *Advances in Atomic and Molecular Physics*, edited by D.R. Bates and I. Estermann (Academic Press, New York, 1966), Vol. 2, p. 177
16. R.I. Hall, L. Avaldi, G. Dawber, P.M. Rutter, M.A. MacDonald, G.C. King, J. Phys. B **22**, 3205 (1989)
17. A.A. Wills, A.A. Cafolla, F.J. Curell, J. Comer, A. Svensson, M.A. MacDonald, J. Phys. B **22**, 3217 (1989)
18. S. Cvejanović, G.W. Bagley, T.J. Reddish, J. Phys. B **27**, 5661 (1994)
19. A. Kikas, S.J. Osborne, A. Ausmees, S. Svensson, O.P. Sairanen, S. Aksela, J. Electron Spectrosc. Relat. Phenom. **77**, 241 (1996)
20. K. Jørgensen, N. Andersen, J. Østgaard Olsen, J. Phys. B **11**, 3951 (1978)
21. G.C. King, M. Tronc, F.H. Read, R. Bradford, J. Phys. B **10**, 2479 (1977)
22. J.J. Jureta, B.P. Marinković, A.R. Milosavljević, L. Avaldi, Eur. Phys. J. D **69**, 74 (2015)
23. J.J. Jureta, A.R. Milosavljević, B.P. Marinković, Int. J. Mass. Spectrom. **365–366**, 114 (2014)
24. R.P. Madden, K. Codling, Phys. Rev. Lett. **10**, 516 (1963)
25. P.J. Hicks, J.M. Sharp, J. Comer, F.H. Read, in *Proceedings of VIII International Conference of Physics of Electronic and Atomic Collisions,* edited by B.C. Čobić and M.V. Kurepa (Institute of Physics, Belgrade, 1973), p. 515
26. S. Svensson, B. Eriksson, N. Martensson, G. Wendin, U. Gelius, J. Electron Spectrosc. Relat. Phenom. **47**, 327 (1988)
27. R.J. Tweed, F. Gelebart, J. Peresse, J. Phys. B **9**, 2643 (1976)
28. B.A. deHarak, J.G. Childers, N.L.S. Martin, Phys. Rev. A **74**, 032714 (2006)
29. J.W. McConkey, J.A. Preston, J. Phys. B **6**, L138 (1973)
30. D.G. Wilden, P.J. Hicks, J. Comer, J. Phys. B **10**, 1477 (1977)
31. B.P. Marinković, J.J. Jureta, A.R. Milosavljević, J. Phys. Conf. Ser. **635**, 052033 (2015)
32. M.O. Krause, S.B. Whitfield, C.D. Caldwell, J.Z. Wu, P. van der Meulen, C.A. de Lange, P.W.C. Hausen, J. Electron Spectrosc. Relat. Phenom. **58**, 79 (1992)
33. L. Minnhagen, J. Opt. Soc. Am. **61**, 1257 (1971)
34. L. Minnhagen, Ark. Fys. **25**, 203 (1963)
35. M.Y. Adam, F. Wuilleumier, S. Krummacher, V. Schmidt, W. Mehlhorn, J. Phys. B **11**, L413 (1978)
36. H.W. Dassen, R. Gomez, G.C. King, J.W. McConkey, J. Phys. B **16**, 1481 (1983)